ROTATIONAL SINGLE SHEET TESTERS FOR MULTI-PARAMETRIC TESTING OF SOFT MAGNETIC MATERIALS - A REVIEW

Helmut Pfützner

Inst. of Fundamentals and Theory of Electrotechnics, Bioelectricity & Magnetism Lab.
Vienna University of Technology, Gusshausstr.27, A-1040 Vienna
Phone (+43)1-58801-35115, Fax (+43)1-5057940, e-mail pfutzner@gte.tuwien.ac.at

Abstract - *During the last decades, a variety of so-called Rotational Single Sheet Testers (RSSTs) have been developed for multi-parametric investigations of laminated soft magnetic materials (e.g., silicon iron sheets or amorphous ribbons) under two-dimensional magnetization. The present paper reviews (i) the practical relevance of rotational magnetization (RM), (ii) designs of RSSTs for the simulation of RM, (iii) the establishment of multi-directional permeability data, (iv) the corresponding power losses, and (v) the measurement of multi-directional magnetostriction.*

Keywords - *Soft magnetic materials, rotational magnetization, power loss measurement, magnetostriction measurement.*

1. INTRODUCTION

During the last two decades, a variety of so-called Rotational Single Sheet Testers (RSSTs) have been developed for multi-parametric investigations of laminated soft magnetic materials. Meanwhile, RSSTs are applied in many academic and industrial institutions for the simulation of so-called rotational magnetization. Per definition, the latter is given in all those cases where the induction vector $\boldsymbol{B}$ shows the phenomenon of rotation during a cycle of dynamic magnetization.

Rotational magnetization arises in a most common way in 3-phase excited electric machines. For example, Fig.1a (after [1]) shows induction time patterns $\boldsymbol{B}(t)$ as being typical for T-joints of transformer cores assembled from highly grain oriented silicon iron sheets. Due to very high anisotropy, the material tends to show rhombic patterns, i.e. the modulus B shows a maximum when passing through the material´s easy direction (the rolling direction r.d.), a relative maximum for the transverse direction (t.d.) and a minimum for the "hard direction" (e.g. 50° to the r.d.). Fig.1b (after [2]) shows patterns as being typical for rotating machines assembled from non-oriented materials (crystalline silicon iron; or amorphous ribbons, i.e. "magnetic glasses"). Due to lacking anisotropy, we see elliptical patterns or even circular ones.

Apart from its scientific attractiveness, rotational magnetization shows high practical relevance due to the fact that it tends to be linked with strong increases of magnetic power losses. For example, a local "building factor" b up to 2.43 is given in Fig.1a which means that the corresponding region exhibits 143% excess loss (compared to the outer limb regions which show pure alternating magnetization in approximation). Apart from loss increases, recent studies have shown that rotational magnetization may cause dramatic increases of magnetostriction. In [3], we demonstrated that the magnetostriction-caused strain l may increase by a factor 100. In spite of local phenomena, the core vibration - and thus also the audible noise - may increase in a distinct way. This is of high practical relevance considering the gradually increasing environmental consciousness.

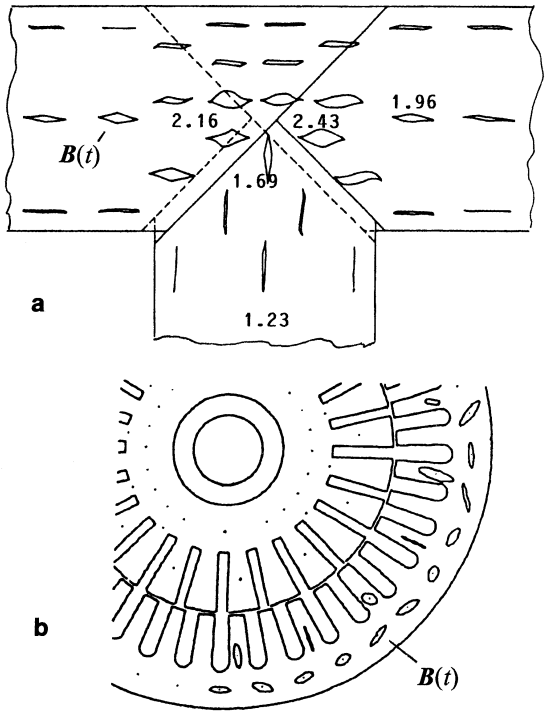

Figure 1 - Examples of practically relevant time patterns $\boldsymbol{B}(t)$ of the induction vector. (a) T-joint of a transformer core; the numbers indicate the local building factor b (after [1]). (b) Yoke of a rotating machine (after [2]).

Rotational magnetization patterns depend on many parameters in a complex way. Thus numerical simulation is very difficult, or even impossible in the case of strongly textured materials. Direct experimental measurement in situ tends to be complicated due to restricted access to the affected core regions of operated machines. This means that experimental simulation by means of specifically designed RSSTs is the most effective way for the collection of both data and deeper physical understanding. The following offers a short review about test apparatuses and their results.

ISBN 972-98115-4-7

2. ROTATIONAL SINGLE SHEET TESTERS (RSSTs)

The basic elements of RSSTs are taken over from conventional test apparatuses for soft magnetic materials as schematically shown in Fig.2. Fig.2a shows the well known principle of standardized single sheet testers (SSTs [4,5]), where a large, square sample (usually 500 mm x 500 mm) is magnetized by the two pole faces of a yoke characterized by large cross section. This yields alternating magnetization in r.d. Exact sinusoidal course of time $B(t)$ can be attained by feed back methods. Fig.2b shows a so-called strip tester which yields an induction vector $\boldsymbol{B}(t)$ in strip direction, i.e. in an angle y to the r.d. During a cycle of magnetization, the corresponding field vector $\boldsymbol{H}(t)$ will show changes of both momentum and direction. Such testers have been applied for several decades for studies of permeability, losses and magnetostriction. However, they show two significant drawbacks: (i) Pure alternating magnetization out of the easy direction is not likely to arise in practice. (ii) The determination of vector interdependencies $\boldsymbol{B}(\boldsymbol{H})$ is very time consuming since n samples are needed for n values of y . On the other hand, an RSST yields $\boldsymbol{B}(\boldsymbol{H})$ and magnetostriction within shortest time by means of a single sample.

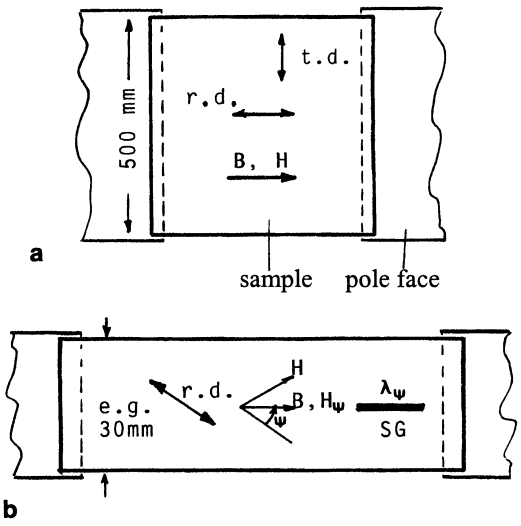

Figure 2 - Apparatus yielding data on alternating magnetization.
(a) Single sheet tester (SST) for magnetization in rolling direction (r.d.).
(b) Strip tester for magnetization in different angles y to the r.d.
(SG strain gauge yielding MS-caused strain l_y).

The main task of an RSST is to magnetize a sample of material in a well defined rotational way and to determine a variety of physical characteristics which may comprise the following:

- the induction time pattern $\boldsymbol{B}(t)$
- the field time pattern $\boldsymbol{H}(t)$
- the power losses P
- the magnetostriction-caused strain in the sample plain x, y and in normal direction z as a function of time, i.e. $l(x,y,z,t)$
- the domain configuration as a function of time.

For the determination of the above characteristics, several versions of apparatus have been developed [6]. Most techniques use a square sample (e.g., 80mm x 80mm) magnetized according to Fig.3a by means of two excitation units arranged in r.d. and t.d., corresponding to excitation voltages U_R and U_T, respectively. The most common target is to simulate circular magnetization in the central sample region. However, in principle, the method can be used to produce patterns $\boldsymbol{B}(t)$ of arbitrarily defined shape, including alternating magnetization, or patterns according to Fig.1. The main practical problem is to establish controlled time changes $U_R(t)$ and $U_T(t)$ by means of specific feedback designs. These specific requirements make it clear why such controlled RSSTs are not available in a general way.

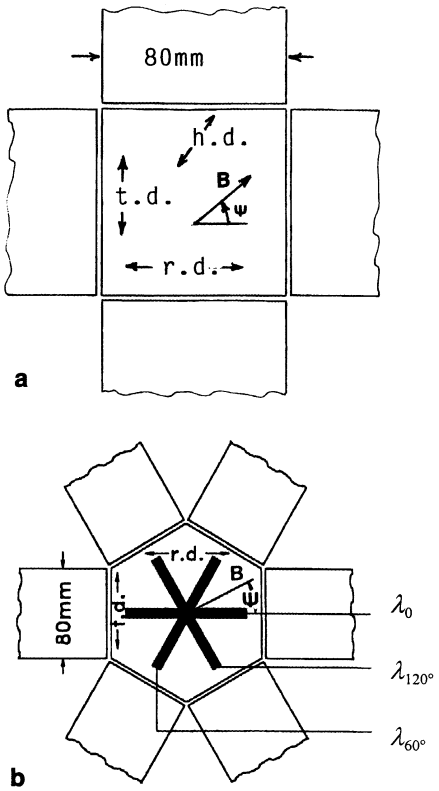

Figure 3 - "Rotational" single sheet testers (RSSTs) for studies of multi-directional magnetization.
(a) 2-phase excited apparatus. (b) 3-phase excited apparatus.

In principle, the above described excitation device represents a 2-phase system. On the other hand, magnetization patterns as shown in Fig.1 tend to arise in electric machines which are excited by 3-phase voltages. The latter fact stimulated the design of an RSST which is excited in a 3-phase mode according to Fig.3b [7-11]. Investigations are made on a hexagonal sample of about 16 cm mean diameter. Well defined patterns $\boldsymbol{B}(t)$ of arbitrary shape can be produced in about one minute by means of a Fuzzy logic algorithm (Fig.4; [8]). However, patterns as arising in practice can be simulated in good approximation by means of generally available 3-phase mains due to close analogy with technical conditions. Replacing specific control electronics by three

auto-transformers yields a simple and robust test apparatus which can be applied in a versatile way.

As demonstrated in the following, RSSTs represent an effective and rapid source of numerical data for all three permeability, losses and magnetostriction.

3. MULTIDIRECTIONAL PERMEABILITY DATA

As a starting point, let us assume that e.g. the finite element method should be used to model the 2-D flux distribution in a soft magnetic device, e.g. the T-joint region of a transformer core built up from anisotropic material (Fig.1a). For its characterization, a permeability tensor [12] has to be established. For permeability data as expressed through $\boldsymbol{B}(\boldsymbol{H})$, RSSTs are equipped with two tangential field coils (usually on a common core) arranged in r.d. and t.d., respectively. The two coil voltages are proportional to $H'_{\text{r.d.}}(= \mathrm{d}H_{\text{r.d.}}/\mathrm{d}t)$ and $H'_{\text{t.d.}}$ thus yielding the field vector $\boldsymbol{H}$ averaged over the e.g. 5cm x 5cm central sample region. The corresponding vector $\boldsymbol{B}$ can be determined by means of two search coils or - much more simple - by two needle contact pairs at the sample bottom (e.g., [7,13]), their voltages $U_{\text{r.d.}}$ and $U_{\text{t.d.}}$ being proportional to $B'_{\text{r.d.}}$ and $B'_{\text{t.d.}}$, respectively. To reduce errors due to sensor imperfection, it is recommended to confirm the correspondence $B_{\text{r.d.}}(H_{\text{r.d.}})$ for alternating magnetization by means of SST (compare Section 4).

Fig.5 (after [9]) shows typical results of measurement for the case of rotational magnetization. The graphic includes four lozenge-like induction patterns with different peak values $B_{\text{r.d.}} \approx B_{\text{t.d.}}$ (note: saturation arises close to 2 T). The given $\boldsymbol{B}(\boldsymbol{H})$-data concerns the steady-state case of rotational magnetization at 50 Hz, being influenced by mechanisms of hysteresis and eddy currents. As closer discussed in [13], these two phenomena yield a lag of $\boldsymbol{B}$ behind $\boldsymbol{H}$ superimposed to effects of anisotropy. This explains that there arises a butterfly-like H-curve of distinctly asymmetric shape, the correspondence between $\boldsymbol{B}(t)$ and $\boldsymbol{H}(t)$ being a characteristic of the entire cycle of magnetization.

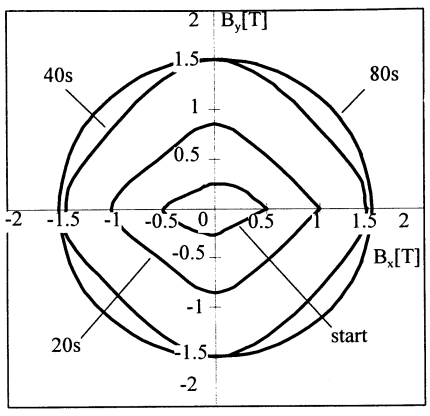

Figure 4 - Approximation of circular magnetization of highly grain oriented SiFe by means of Fuzzy logic control. The procedure starts with weak lozenge-like magnetization. The target of constant $B = 1.5$ T in all directions is reached after 80 s [8].

The definition of 2-D permeability values analogous to those as resulting, e.g., from a 1-D virgin curve is ambiguous a priori due to the infinite number of possible magnetic histories. However, data for numerical modeling are offered by vector equivalencies $\boldsymbol{B}(\boldsymbol{H})$ for different values of y . Fig.6 illustrates this procedure using the example of an elliptical B-pattern under different conditions of mechanical stress s (after [10]). Within the half period, equivalencies are marked for 13 instants of time, according to a corresponding computer data file. A possible way for the estimation of equivalencies of the whole plane is offered by 2-D interpolation, e.g. by means of artificial neural networks as discussed in [11].

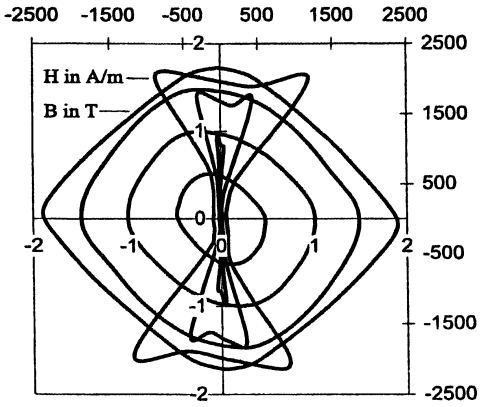

Figure 5 - Typical example for $\boldsymbol{B}(\boldsymbol{H})$ data for h.g.o. SiFe magnetized lozenge-like with different peak values $B_{\text{r.d.}} \approx B_{\text{t.d.}}$ (after [9]). $\boldsymbol{B}$ passes through the "hard direction" (h.d.) for y close to 55° corresponding to maximum H at the same instant.

4. POWER LOSS DETERMINATION

A very simple way to determine total power loss (in W/kg) is given by means of the well known formula

$$P = 1/(r\,T) \cdot {}_{\text{T}}\!\int \boldsymbol{H}(t) \cdot \boldsymbol{B}'(t)\,\mathrm{d}t \qquad (1)$$

(T period, r density in kg/m³). As closer discussed in [13], this formula yields mere hysteresis losses if $\boldsymbol{H}$ and $\boldsymbol{B}'$ (= $\mathrm{d}\boldsymbol{B}/\mathrm{d}t$) are averaged over the sample's cross section as being typical for quasi-static conditions. On the other hand, RSST results which are derived dynamically (e.g. for 50 Hz) yield $\boldsymbol{H}$ on the sample *surface* while $\boldsymbol{B}$ represents the induction averaged over the cross section. This means that the correspondence $\boldsymbol{B}(\boldsymbol{H})$ (e.g., Fig.6) comprises a priori also eddy current effects.

An alternative is to determine the total loss by means of the well known rise of temperature technique [14] arranging a thermistor at the sample center. However wide experimental experience from both methods shows that RSSTs cannot be used to obtain quantitatively exact loss data. A European intercomparison of measurements performed in six labs yielded differences of the order 20% [15] which can be explained by inhomogeneous flux, insufficient calibration of search coils or thermistors, and others. It can be concluded that RSSTs are unsuited to determine absolute loss values

while they are a very effective tool to determine relative differences.

Considering the above situation, we suggest to express the result as a "related loss increase"

$$p = P / P_{\text{r.d.}} \quad , \qquad (2)$$

analogous to the definition of the local building factor

$$b = P_{\text{local}} / P_{\text{SST}} \qquad (3)$$

of a magnetic core (with P_{local} the local loss value and P_{SST} determined by standardized SST method).

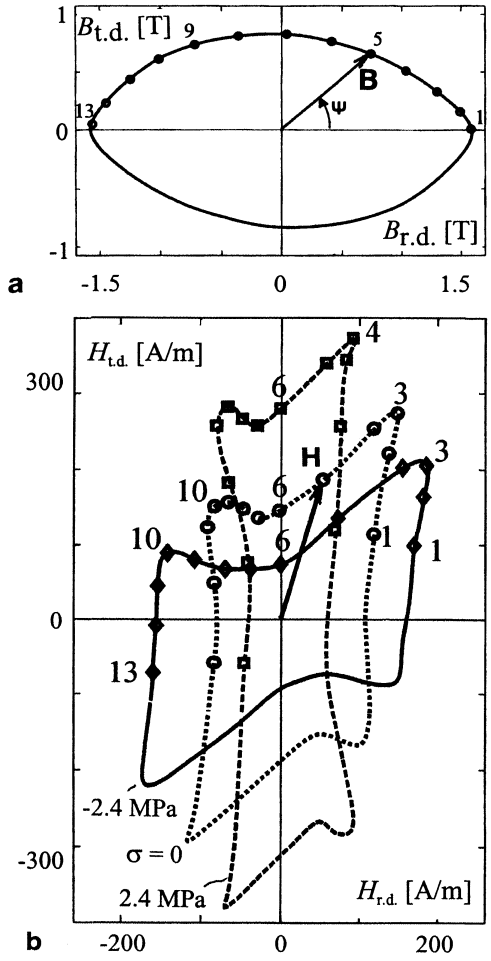

Figure 6 - ***B***(***H***) data for elliptically magnetized h.g.o. SiFe for different states of mechanical stress s [10]. (a) Time-pattern of the induction vector ***B*** (axis ratio $a = B_{\text{t.d.}}/B_{\text{r.d.}} = 0.53$). (b) Corresponding patterns of the field vector ***H***. Note: 1..13 mark time instants of constant interval and thus define the vector correspondencies (as sketched for instant 5; $s = 0$).

For example, the case of elliptical magnetization (unstressed state $s = 0$) in Fig.6 yielded $p = 2.23$, i.e. 123% loss increase compared to $P_{\text{r.d.}}$ for 1.5 T [10]. The use of p allows a direct comparison between this RSST result and the local building factor b as included into Fig.1a. The center of the T-joint region shows very similar values b (2.16, 2.43) corresponding to magnetization patterns of similar $B_{\text{r.d.}}$ and axis ratio a .

The above example of a comparison between the result of an RSST simulation and the result of an experimental core investigation shows very good agreement - probably by chance, if we consider the scatter of losses as being typical for different charges of material. Further, core losses may be increased due to many factors such as mechanical stress. In the case of Fig.6, tensile stress (s = 2.4 MPa) yielded p = 2.70, while the compressive state (s = -2.4 MPa) proved to be less disadvantageous according to p = 2.47.

It can be concluded from the above that loss predictions by means of simulation or numerical modeling will show considerably high errors *a priori* if multidirectional magnetization is involved. However, it should be considered that even 1-D testing by means of standardized SSTs may show errors up to 10% [16]. Thus, in the RSST-case, orders of 20% are still acceptable for practice. Loss increases due to 2-D conditions tend to be very large, higher uncertainties thus being tolerable.

5. MAGNETOSTRICTION MEASUREMENT

As already mentioned, the RSST sample can also be used to establish data on multi-directional magnetostriction (MS). As shown by Fig.3b, three strain gauges or three laser interference sensors, respectively, are applied to detect MS-caused strain in three directions of the sample plane in order to calculate the strain tensor. While details are given elsewhere [3, 9-11], in the following a result of measurement is used to demonstrate the high significance of RSST for global core vibrations and the corresponding noise levels.

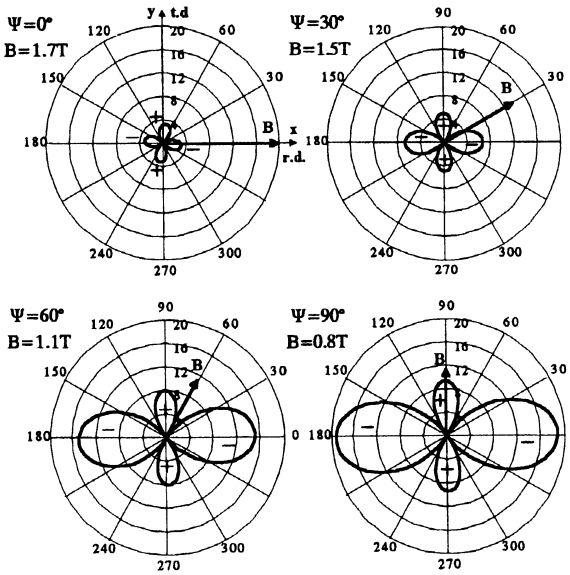

Figure 7 - MS-caused strain l (in µm/m) in all directions of the sample plane for elliptical magnetization (a = 0.47). The four graphs show "strain snapshots" for four instants of time during a quarter period (after [3]).

Fig.7 shows MS-caused strain l for elliptical magnetization according to Fig.6, although for higher $B_{\text{r.d.}}$ (1.7T instead of 1.5T, i.e. axis ratio a = 0.47 instead of 0.53). Out

of a period of magnetization, four "strain snapshots" are shown related to the demagnetized case: The instant of time of $\boldsymbol{B}$ in r.d. (y = 0) yields slight shrinking ($l_{\text{r.d.}}$ = - 3μm/m) in r.d. which is compensated by elongation in t.d. (apart from an additional sheet thickness increase). These tendencies become more distinct with increasing y. For the instant y = 90°, the strain in r.d. reaches $l_{\text{r.d.}}$ = -19 μm/m, the practically relevant peak-to-peak value thus resulting as $l_{\text{r.d.,pp}}$ = -19 μm/m + 3 μm/m = -16 μm/m. Analogous, the graphs offer data for all other directions. For example, for t.d. we find $l_{\text{t.d.,pp}}$ = 10 μm/m - 3 μm/m = 7 μm/m.

It should be stressed that the above data can be derived from a single period of rotational magnetization with very short procedure time. But analogous to permeability, an abundance of data results which needs effective management. Strategies to reduce the number of stored data are offered by interpolation techniques based on statistics. As a possible alternative, we checked the effectiveness of artificial neural networks [11]. They prove to yield effective interpolation, provided that well distributed training data - established by continuously performed experimental measurements - is given.

7. CONCLUSIONS

The main conclusions of this study are the following:

(1) Rotational magnetization patterns can be produced by means of "rotational" single sheet testers (RSSTs) which use two or three yokes for the magnetization of a sample of material of square or hexagonal shape, respectively.

(2) RSSTs can be used for all types of laminated soft magnetic materials, three yoke techniques being advantageous in the case of h.g.o. SiFe of high anisotropy.

(3) Compact sensor sets yield simultaneous information on permeability, losses and magnetostriction (MS).

(4) For numerical modeling of 2-D flux distributions, RSSTs offer interdependencies between the induction vector $\boldsymbol{B}$ and the field vector $\boldsymbol{H}$.

(5) Modeling of 2-D loss distributions through post-processing is favored by data on p, i.e. total losses related to losses for $\boldsymbol{B}$ in rolling direction (r.d.) (in equivalence to the "local building factor" b of magnetic cores).

(6) MS-caused strain l in all directions of the sample plane and normal to it can be determined by means of three strain gauges arranged in three different directions.

(7) Specific problems arise from the fact that the high variety of 2-D magnetization patterns yields a high abundance of data. Restrictions can be attained by interpolation procedures, e.g., using artificial neural networks.

The aim of this paper was to demonstrate the high RSST-potential to supply information of physical and industrial relevance. Closer details are given by a very high amount of papers published in [6].

ACKNOWLEDGEMENT

The author thanks for support from the Austrian FWF (Project P10968-PHY), from ABB Transformers (Ludvika, Sweden), and from ABB Power T&D (St.Louis, USA).

REFERENCES

[1] "Electrical Steel Sheets - Orientcore HI-B". *Nippon Steel Corporation Product Catalogue*.

[2] M.Enokizono, S.Fujiyama: "The influence of compressive stress on the magnetic flux density in a 3-phase induction motor core model". *J.Phys.IV France* 8, Pr2 801-804 (1998).

[3] A.Hasenzagl, B.Weiser, H.Pfützner: "Magnetostriction of 3% SiFe for 2-D magnetization patterns". *J.Magn.Magn.Mater.*160, 55-56 (1996).

[4] "Methods of measurement of specific total losses of magnetic sheet and strip by means of single sheet tester". *IEC Publ.*404-3 (1982).

[5] "Methods of measurement of magnetic properties of magnetic sheet and strip by means of a single sheet tester". *IEC Publ.*404-3 (1992).

[6] A very high number of publications in *Procs.Int.Workshops on 2-D Magnetization Problems*: Braunschweig (1991), Oita (1992), Torino (1993), Cardiff (1995), Grenoble (1997), Bad Gastein (2000).

[7] A.Hasenzagl, B.Weiser, H.Pfützner: "Novel 3-phase excited single sheet tester for rotational magnetization". *J.Magn.Magn.Mater.*160, 180-182 (1996).

[8] A.Hasenzagl, H.Pfützner, A.Saito, Y.Okazaki: "Fuzzy logic control system for the excitation of a 3-phase single sheet tester". *J.Phys.IV France* 8, Pr2 685-688 (1998).

[9] A.Hasenzagl, H.Pfützner, A.Saito, Y.Okazaki: "Status of the Vienna hexagonal single sheet tester". *Proc.5th Int.Workshop on 2-D Magnetization Problems* Grenoble (Ed.A.Kedous-Lebouc), 33-41 (1997).

[10] C.Krell, N.Baumgartinger, G.Krismanic, H.Pfützner: "Stress effects on the multidirectional behavior of g.o. silicon iron sheets". *J.Magn.Magn. Mater.*215-216, 63-65 (2000).

[11] N.Baumgartinger, A.Hasenzagl, H.Pfützner, G.Krismanic: "Application of neural networks for the prediction of multi-directional magnetostriction". *J.Magn.Magn. Mater.*215-216, 617-619 (2000).

[12] W.Brix, K.A.Hempel: "Tensorial descriptions of the rotational magnetization process in anisotropic silicon steel". *J.Magn.Magn. Mater.*41, 279-281 (1984).

[13] H.Pfützner: "Rotational magnetization and rotational losses of g.o. Si steel sheets - Fundamental aspects and theory". *IEEE Trans.Magn.*30, 2802-2807 (1994).

[14] F.Fiorillo: "On the measurement of rotational losses by means of the rise of temperature technique". *IEC Publ.*TC68 WG2 N58 (1990).

[15] J.Sievert, H.Ahlers, M.Birkfeld, B.Cornut, F.Fiorillo, K.A.Hempel, T.Kochmann, A.Kedous-Lebouc, T.Meydan, A.Moses, A.M.Rietto: "European intercomparison of measurements of rotational power loss in electrical sheet steel". *J.Magn.Magn.Mater.*160, 115-118 (1996).

[16] R.S.Girgis, K.Gramm, J.Sievert, M.G.Wickramasekara: "The single sheet tester. Its acceptance, reproducibility, and application issues on grain-oriented steel". *J.Phys.IV France* 8, Pr2 729-732 (1998).